Image multiplying and high-frequency oscillations effects in the Fresnel region light propagation simulation

Maciej Sypek
Czesław Prokopowicz
Michal Górecki, MEMBER SPIE
Warsaw University of Technology
Faculty of Physics
Koszykowa 75
PL-00-662, Warsaw, Poland
E-mail: sypek@if.pw.edu.pl

Abstract. A new effect during light propagation simulation in the Fresnel region is discovered. Image multiplying and high-frequency noise effects are caused by the sampling of the complex light field. Image multiplying is observed in the case of the standard integral calculation. High-frequency noise is observed in the convolution approach. These effects are observed in a computer simulation only and do not exist in nature. The analysis of these effects enable us to define the range of the numerical algorithms application. © *2003 Society of Photo-Optical Instrumentation Engineers.* [DOI: 10.1117/1.1613959]

Subject terms: diffractive optics; propagation; digital processing.

Paper 030010 received Jan. 7, 2003; revised manuscript received Apr. 1, 2003; accepted for publication May 1, 2003.

1 Introduction

In digital holography, the light propagation phenomena is usually simulated and calculated by means of a computer. A Fresnel hologram reconstructs a signal at a finite distance behind the hologram plane. In comparison to digital Fourier holography, the effort to calculate a Fresnel hologram is comprehensive.

During computer simulations, sampling of the light field is always necessary. This paper describes image multiplying and high-frequency oscillation effect caused by sampling. Numerical methods are essential tools in digital holography. They enable us to design synthetic holograms. The mentioned methods can be also applied for light field reconstruction simulations from structures designed in other ways—ray tracing or the stationary phase method.[1,2] However, some traps are included in the computer algorithms. It is possible to find some effects that can appear in numerical approach but that do not exist in nature. We provide some suggestions on how to avoid these traps.

Direct practical application of the Fresnel formula[3–5] is useful for numerical simulation of light propagation, but for a large distance only. Thus, this method is not very useful in the Fresnel region. For a small distance between an object and the hologram plane, the Fresnel factor reveals fast oscillations. The Fresnel factor can be interpreted as a divergent spherical lens. If the sampling frequency is insufficient or the distance is to small, the lens will be multiplied.[6–9] This effect leads to multiplication of the light field. If the diffraction image is limited, it is easily possible to find multiplied images. In the opposite case, the interference of the multiplied images will completely disturb the Fresnel diffraction field.

Another approach to the numerical simulation of the light propagation in the Fresnel region is decomposition of the field amplitude into the plane waves.[10–14] In this case, we can describe the output complex amplitude as the convolution of the input distribution and an impulse response function for free space.[10,15] This last function is known in analytical form and exhibits very slow oscillations for a small distance between an object and the hologram plane. However, for an increasing distance (still in the Fresnel region) a lens-like factor will multiply.[6–9] This effect—in the Fourier space—will cause high-frequency oscillations in the Fresnel diffraction image.

2 Sampled Fresnel Lenses

In this section, the effect of the Fresnel lens multiplication is explained. The superimposing of the Fresnel lens encoded in the sampling grid causes a moiré effect[8] to appear. Such a behavior was previously described.[6,9]

In general, the complex transmittance of the Fresnel lens is written as

$$Z(x,y)=\exp\left[-ik\frac{(x^2+y^2)}{2f}\right], \tag{1}$$

where f is the focal length of the lens and $k=2\pi/\lambda$.

During computer simulations, sampling of such an element is always necessary. We codify this lens in a matrix that contains $N\times M$ pixels with center-to-center spacing $(\Delta x,\Delta y)$. The coordinates of the pixels centres can be written as

$$\begin{aligned} x_n&=[n+\tfrac{1}{2}P(N)]\Delta x, \quad n=0,\pm 1,\pm 2,\ldots,\\ y_m&=[m+\tfrac{1}{2}P(M)]\Delta y, \quad m=0,\pm 1,\pm 2,\ldots, \end{aligned} \tag{2}$$

where $P(N)$ is a parity function

$$P(N)=\begin{cases} 0 & \text{odd } N\\ 1 & \text{even } N \end{cases}. \tag{3}$$

 © 2003 Society of Photo-Optical Instrumentation Engineers

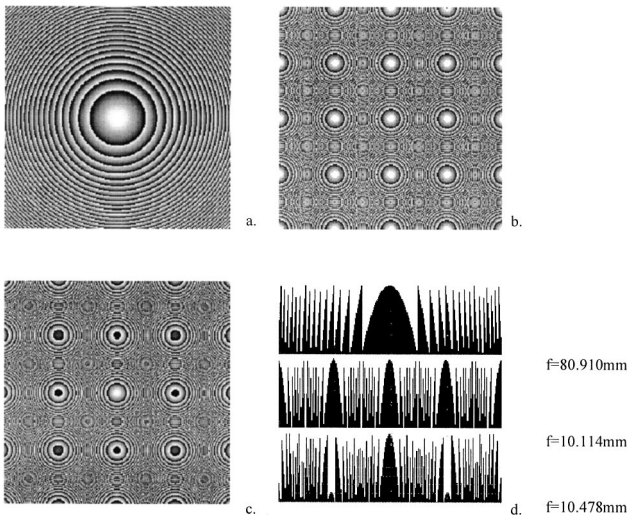

Fig. 1 Numerically calculated phase of the encoded Fresnel lens with focal length f, $N=M=256$, and $\Delta x=\Delta y=0.01$ mm, where (a) $f=80.910$ mm gives $R_x=R_y=5.12$ mm (multiplied lenses "are placed outside the area"), (b) $f=10.114$ mm gives $R_x=R_y=0.64$ mm [lens (x_k,y_l) coincides with the center of the pixel), and (c) $f=10.478$ mm gives $R_x=R_y=0.663$ mm [lens (x_k,y_l) does not coincide with the center of the pixel]. (d) Respectively, phase cross section in the center of each picture. Note that in 2-D bit maps white corresponds to a phase of 2π and black corresponds to 0. The range of the phase cross section is 0 to 2π.

The codification involves a sampling process of the Fresnel lens by means of multiplication with a 2-D comb[16] function with spacing $(\Delta x,\Delta y)$. Sampling of the convergent spherical wave leads to the multiplication of the focal points in the focal plane. New foci appear in the following coordinates;

$$x_k=kX, \quad X=\frac{\lambda f}{\Delta x}, \quad k=0,\pm 1,\pm 2,\ldots,$$
$$y_l=lY, \quad Y=\frac{\lambda f}{\Delta y}, \quad l=0,\pm 1,\pm 2,\ldots. \tag{4}$$

The distances R_x and R_y in pixels between the foci can be easy calculated. We call (k,l) the order of lens.[6]

$$R_x=\frac{X}{\Delta x}, \quad R_y=\frac{Y}{\Delta y}. \tag{5}$$

Thus, in the image plane, the encoded lens behaves as an array of lenses centered in coordinates (x_k,y_l). Note the following problems in our further considerations. The center of the higher order lens (x_k,y_l) does not usually coincide with the center of the pixel.

The factor $Z(x-kX,y-lY)$ appears as a (k,l)-order Fresnel lens with focal lens f. Depending on indices k and l it is shifted from the original position. Moreover, a single lens has an additional, constant phase shift $\exp(i\phi_{k,l})$ (Ref. 6). As already mentioned, the center of the higher order lens (x_k,y_l) does not usually coincide with the center of the pixel. Codification of the Fresnel lens is described in Fig. 1.

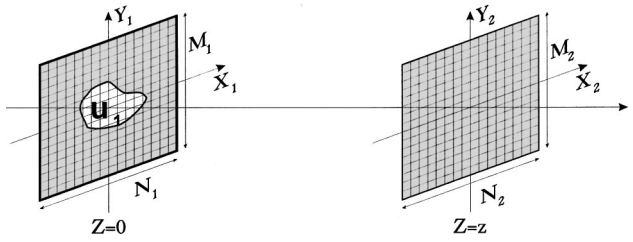

Fig. 2 Optical setup for the numerical analysis.

3 Direct Theoretical Approach

The amplitude and phase distribution $u_2(x_2,y_2)$ in the plane at the distance z behind the input plane is expressed by the integral based on the Fresnel approximation.

$$u_2(x_2,y_2)=\frac{\exp(ikz)}{i\lambda z}\int\int_{-\infty}^{+\infty} u_1(x_1,y_1) \times\exp\left\{\frac{ik}{2z}[(x_1-x_2)^2+(y_1-y_2)^2]\right\}\mathrm{d}x_1\,\mathrm{d}y_1. \tag{6}$$

Input signal $u_1(x_1,y_1)$ is illuminated by a plane wave with wavelength λ $(K=2\pi/\lambda)$. Equation (6) can be rewritten in the following form, where Fresnel factor appears.

$$u_2(x_2,y_2)=\frac{\exp(ikz)}{i\lambda z}\exp\left[\frac{ik}{2z}(x_2^2+y_2^2)\right] \cdot\int\int_{-\infty}^{+\infty} u_1(x_1,y_1)\exp\left[\frac{ik}{2z}(x_1^2+y_1^2)\right] \times\exp\left[-\frac{ik}{z}(x_1x_2+y_1y_2)\right]\mathrm{d}x_1\,\mathrm{d}y_1. \tag{7}$$

From the numerical point of view we consider optical setup shown in Fig. 2. Input plane X_1, Y_1 with signal $u_1(x_1,y_1)$ is encoded in a matrix of $N_1\times M_1$ complex points. Sampling distances in this plane are equal to $(\Delta x_1,\Delta y_1)$. Then we calculate light complex amplitude distribution $u_2(x_2,y_2)$ in the plane X_2, Y_2. The last mentioned distribution is also encoded in a matrix of $N_2\times M_2$ complex points with sampling distances $(\Delta x_2,\Delta y_2)$.

Application of the numerical algorithm to the preceding problem leads us to the following formula based on Eq. (7) [written for the case where parity function $P(N_1)=P(M_1)=P(N_2)=P(M_2)=0$].

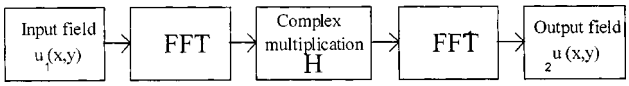

Fig. 3 Convolution approach algorithm.

$$
\begin{aligned}
&u_2(n_2\Delta x_2, m_2\Delta y_2)\\
&\quad=\frac{\exp(ikz)}{i\lambda z}\exp\left\{\frac{ik}{2z}[(n_2\Delta x_2)^2+(m_2\Delta y_2)^2]\right\}\\
&\quad\times\sum_{n_1=1}^{N_1}\sum_{m_1=1}^{M_1}u_1(n_1\Delta x_1, m_1\Delta y_1)\\
&\quad\times\exp\left\{\frac{ik}{2z}[(n_1\Delta x_1)^2+(m_1\Delta y_1)^2]\right\}\\
&\quad\times\exp\left[-\frac{ik}{z}(n_1\Delta x_1 n_2\Delta x_2+m_1\Delta y_1 m_2\Delta y_2)\right]\Delta x_1\Delta y_1 .
\end{aligned}
\tag{8}
$$

Note here that general theory [see Eq. (7)] requires the following condition to be fulfilled for Fresnel region[4,15]:

$$
z^3 \gg \frac{\pi}{4\lambda}[(x_0-x_1)^2+(y_0-y_1)^2]^2_{\max}. \tag{9}
$$

However, this requirement is in general not necessary for the Fresnel approximation to remain valid.[15] The Fresnel approximation gives accurate results for diffraction angles[17] up to 18 deg.

By futher analysis of Eq. (8) we find the next, serious limitation. The distance parameters z of the lens-like factors are placed in the denominators of the fractions. Small values of z yield large phase values of the lens-like factors, which exhibit rapid oscillations. If distance z is to small in comparison to sampling distances $(\Delta x_1, \Delta y_1)$ or $(\Delta x_2, \Delta y_2)$ the moiré effect appears. Lens-like factors will multiply.

Note that an image multiplacation effect will not appear (in the analyzed area) if the following condition for distance z is fulfilled:

$$
N_1\Delta x_1 < \frac{\lambda z}{\Delta x_1} \Rightarrow z > \frac{N_1(\Delta x_1)^2}{\lambda}, \tag{10}
$$

and

$$
M_1\Delta y_1 < \frac{\lambda z}{\Delta y_1} \Rightarrow z > \frac{M_1(\Delta y_1)^2}{\lambda}.
$$

The simplest interpretation of this formula is that the distances between the centers of the multiplied lenses [see Eq. (4)] should be greater than the width of the whole area ($N_1\Delta x_1$ or $M_1\Delta y_1$).

By simultaneously decreasing of the spacing distances and increasing the number of samples we can improve the obtained results. Unfortunately, such an operation will increase computation time. Note also that influence of the neighboring vectors[14,16] is not observed for this case. It is a consequence of the calculation of an integral by classical numerical methods. If we avoid application of the discrete Fourier transform[16] (DFT) or fast Fouriet transform[18] (FFT) algorithms the neighboring vectors will not disturb the simulation results. An additional advantage of the preceding method is the possibility of using the different spacing distances in the input and observation planes. However, application of the direct theoretical approach results in a very long calculation time in comparison to other algorithms based on the FFT. In practice, it can be applied for 1-D cases.

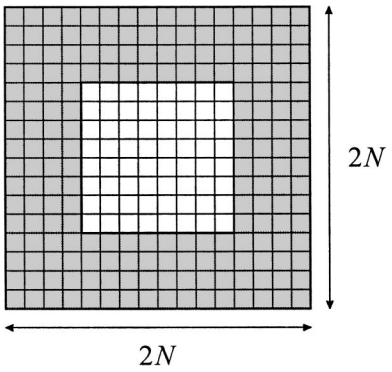

Fig. 4 Modified convolution approach algorithm—embedded area.

4 FFT Application

Another approach to the numerical simulation of the light propagation in the Fresnel region is direct application of the FFT algorithm.

$$
\begin{aligned}
u_2(x_2,y_2)=\frac{\exp(ikz)}{i\lambda z}\exp\left[\frac{ik}{2z}(x_2^2+y_2^2)\right]\\
\times F\left\{u_1(x_1,y_1)\exp\left[\frac{ik}{2z}(x_1^2+y_1^2)\right]\right\},
\end{aligned}
\tag{11}
$$

where $F\{\ldots\}$ is a Fourier transform.

Input signal $u_1(x_1,y_1)$ is illuminated by a plane wave with wavelength λ ($k=2\pi/\lambda$).

In comparison to an analysis of the direct theoretical approach we can find that we have a very similar situation. The main factor $[\exp(ikz)/i\lambda z]\exp[(ik/2z)(x_2^2+y_2^2)]$ is same, so finally for no image multiplying, we get the same condition for distance z:

$$
z > \frac{N_1(\Delta x_1)^2}{\lambda} \quad \text{and} \quad z > \frac{M_1(\Delta y_1)^2}{\lambda}. \tag{12}
$$

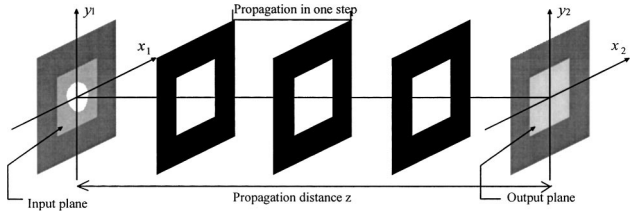

Fig. 5 Modified convolution approach algorithm—multistep propagation.

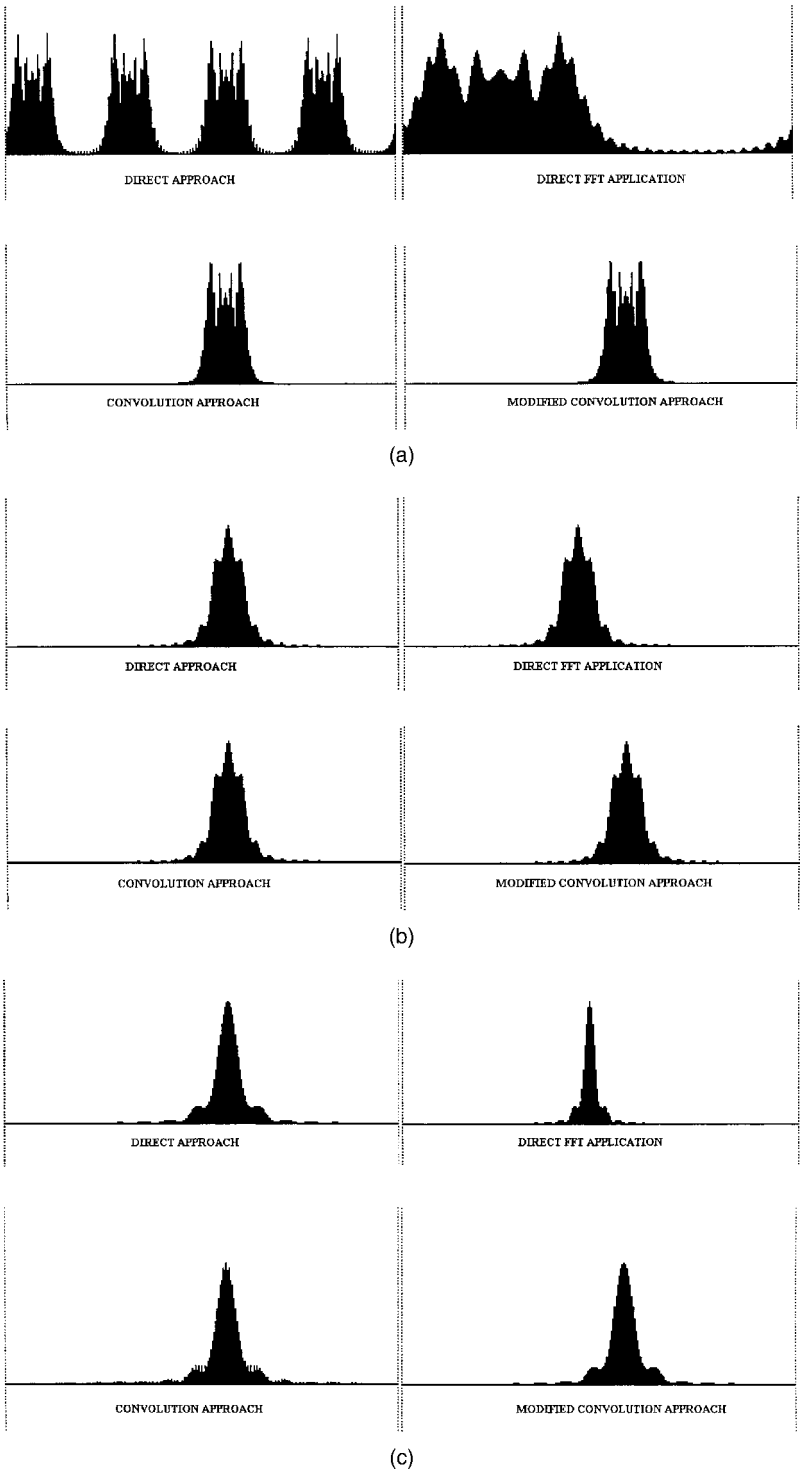

Fig. 6 Computer simulation results for (a) $z=10$ mm ($z<z_0$), (b) critical distance $z=40.455$ mm ($z=z_0$), and (c) $z=80.91$ mm ($z>z_0$).

Additionally, the Fresnel factor $\exp[(ik/2z)(x_1^2+y_1^2)]$ affects rapid oscillations for a small values of z. But these oscillations are observed for a distance z smaller than written in Eq. (12).

The influence of the neighboring vectors[14,16] is observed for this case. It is a consequence of the calculation based on the DFT (Ref. 16) or the FFT (Ref. 18).

5 Convolution Approach

Another approach to the numerical simulation of the light propagation in the Fresnel region is decomposition of the input field amplitude into the plane waves.

By introducing the following notation: $u_1(x_1,y_1)=u_1(x,y)$ and $u_2(x_2,y_2)=u_2(x,y)$ it is possible to write

the output complex field as a convolution of input field and the function $h(x,y)$.

$$u_2(x,y)=u_1(x,y)*h(x,y). \tag{13}$$

The function $h(x,y)$ can be interpreted as a impulse response function in free space for a given distance z.

$$h(x,y)=\frac{\exp(ikz)}{i\lambda z}\exp\left[\frac{ik}{2z}(x^2+y^2)\right]. \tag{14}$$

Based on the convolution theorem,[6] we can write a convolution of two functions in the object space as the product of their Fourier transforms in the Fourier space:

$$U_2(\nu_x,\nu_y)=U_1(\nu_x,\nu_y)H(\nu_x,\nu_y), \tag{15}$$

where

$$U_1(\nu_x,\nu_y)=\Im[u_1(x,y)], U_2(\nu_x,\nu_y)=\Im[u_2(x,y)],$$

where ν_x and ν_y are spatial frequencies.

The Fourier transform of the function $h(x,y)$ can be calculated analytically and is written as follows:

$$H(\nu_x,\nu_y)=\Im[h(x,y)]=\exp(ikz)\exp[-i\pi\lambda z(\nu_x^2+\nu_y^2)]. \tag{16}$$

The mentioned approach has the following interpretation.[15] The input complex amplitude field is decomposed into the plane waves. This first operation corresponds to Fourier transformation. The coherent transfer function H known in the analytical form describes phase retardation of each plane wave. This retardation depends on the propagation angle and the distance z. The output complex amplitude can be obtained as the superposition of the plane waves ''corrected'' by function H. This last operation corresponds to reverse Fourier transformation. Figure 3 presents the algorithm.

Practical application of the described approach is convenient. Both direct and reverse Fourier transformations coordinates in the input (x_1,y_1) and output (x_2,y_2) plane are equivalent. Resampling or interpolation operations are not necessary. Moreover, the phase of the transfer function $H(\nu_x,\nu_y)$/[Eq. (16)] linearly depends on the distance parameter z. For small values of the parameter z, the phase is close to 0 and whole factor reveals very slow oscillations.

Note that the high-frequency oscillation effect will not appear (in the analyzed area) if the following condition for distance z is fulfilled:

$$z\geqslant\frac{1}{\lambda N_1(\Delta v_1)^2}\quad\text{where}\quad\Delta v_1=\frac{\Delta x_1}{\lambda z}, \tag{17}$$

and

$$z\geqslant\frac{1}{\lambda M_1(\Delta v_2)^2}\quad\text{where}\quad\Delta v_2=\frac{\Delta y_1}{\lambda z}.$$

Thus, taking the maximum limitation of Δv_1 and Δv_2 we get the following conditions for distance z depending on the input parameters:

$$z\geqslant\frac{1}{\lambda N_1(\Delta x_1/\lambda z)^2}\Rightarrow z\leqslant\frac{N_1(\Delta x_1)^2}{\lambda}, \tag{18}$$

and

$$z\geqslant\frac{1}{\lambda M_1(\Delta y_1/\lambda z)^2}\Rightarrow z\leqslant\frac{M_1(\Delta y_1)^2}{\lambda}.$$

6 Modified Convolution Approach

Another approach to the numerical simulation of the light propagation in the Fresnel region is the modified convolution approach.[14]

The 1-D propagation is simulated by the convolution of the twice length vector. The influence of the neighboring main processing vectors (length N, white area in Fig. 4) is embedded in another vector (length $2N$, gray area in Fig. 4) of zeros.

This enables us to analize propagation for larger distance z values in one step. In fact, a double size of output field is not exact because we can take, for example, $4x$, $6x$, etc. size of field. The whole propagation distance z can be divided into steps.

This enables us to calculate propagation for any distance z in fewer steps. After every step we must cut the area to the base size of an input area, taking a center (white area in middle planes in Fig. 5).

Thus, for, faster results, we must calculate how large an area we must to take as a calculated area. Simillary to the convolution approach we have the high-frequency oscillations, which can be found for a distance z larger than the maximum distance calculated for one step:

$$z\leqslant\frac{N_1(\Delta x_1)^2}{\lambda}\quad\text{and}\quad z\leqslant\frac{M_1(\Delta y_1)^2}{\lambda}. \tag{19}$$

Thus, in case of a double vector N_1, the distance z will be doubled.

6 One-Dimensional Computer Simulation

For the 1-D example, the following computer simulation was performed in the vector composed of $N_1=256$ complex points. The sampling distance Δx_1 was equal to 0.01 mm. A slit width $d=0.32$ mm was illuminated by a monochromatic plane wave with wavelength $\lambda=0.6328$ μm. The result of the simulation [Figs. 6(a), 6(b), and 6(c)] was stored in a vector composed of $N_2=N_1=256$ complex points. The sampling distance $\Delta x_2=\Delta x_1=0.01$ mm. The calculated critical distance for the preceding parameters is $z_0=40{,}455$ mm.

Figure 6(a) presents simulation results for distance $z=10.0$ mm. For the distance $z<z_0$ the condition of Eq. (10) for the direct theoretical approach is not fulfilled. This causes the image multiplication effect for the direct theoretical approach. For distance $z<z_0$ the condition of Eq. (12) for the direct FFT approach is also not fulfilled. This

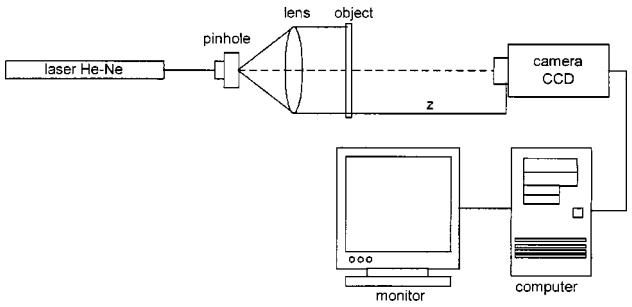

Fig. 7 Experimental setup.

causes diffraction image destruction. Additionally, note that sampling in the output plane is not equal to the input parameters and varies with the z distance for the direct FFT approach. The conditions for the convolution approach and for the modified convolution approach remain fulfilled.

Figure 6(b) presents simulation results for the distance $z=z_0=40.455\,\mathrm{mm}$. All methods are equivalent and return satisfactory results.

Figure 6(c) presents simulation results for the distance $z=2z_0=80.91\,\mathrm{mm}$. For a distance $z>z_0$, the condition of Eq. (18) for the convolution approach is not fulfilled. This causes additional high-frequency oscillation effects for the convolution approach. For the modified convolution approach the condition of Eq. (19) (for doubled N_1 and M_1) is fulfilled.

Additionally note that sampling in the output plane is not equal to the input parameters and varies with the z distance for the direct FFT approach.

7 Two-Dimensional Experimental and Simulation Results

For the 2-D example, the following computer simulation was performed in a matrix composed of $N_1=512\times M_1=512$ complex points. The sampling distance Δx_1 was equal to $\Delta y_1=0.01\,\mathrm{mm}$. A circular aperture with radius $r=1.25\,\mathrm{mm}$ was illuminated by the monochromatic plane wave with wavelength $\lambda=0.6328\ \mu\mathrm{m}$. The result of the simulation was stored in a matrix composed of $N_2=N_1=512\times M_2=M_1=512$ complex points. The sampling distance $\Delta x_2=\Delta x_1=0.01\,\mathrm{mm}$ and $\Delta y_2=\Delta y_1=0.01\,\mathrm{mm}$. The calculated critical distance for the preceding parameters is $z_0=80.91\,\mathrm{mm}$.

Additionally, computer simulation result was verified in the optical setup (Fig. 7). A circular aperture with radius $r=1.25\,\mathrm{mm}$ was illuminated by the monochromatic quasi-plane wave with wavelength $\lambda=0.6328\ \mu\mathrm{m}$. The intensity distribution of the diffractive image at a distance z was captured by CCD camera. The effective pixel in the CCD matrix was the shape of a square with sides $a=0.01\,\mathrm{mm}$.

Figure 8 presents simulation and experimetal results for the distance $z=1234\,\mathrm{mm}$. For distance $z>z_0$ the condition of Eq. (18) for the convolution approach is not fulfilled. This causes additional high-frequency oscillation effects for the convolution approach.

Conditions for the direct theoretical approach for the modified convolution approach with the multistep algorithm (single step equal to $2z_0$) and the direct FFT approach remain fulfilled. Additionally, note that sampling in the output plane is not equal to the input parametes and varies with the z distance for the direct FFT approach. Thus, resampling of the calculated image is necessary.

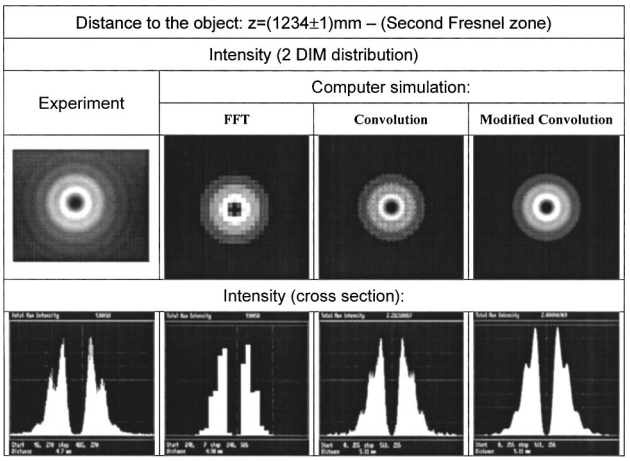

Fig. 8 Experimental and simulation results.

8 Conclusions

The problem of the validity range for the application of the Fresnel approximation is a very old one.[19,20] From the analytical point of view it is possible to calculate the complex amplitude distribution behind the input plane. Paraxial versions of angular spectrum calculations are done in the near field, while Rayleigh-Sommerfeld is done in the far field.[21] However, in digital holography the light propagation phenomena is usually simulated and calculated by means of a computer. This—in the general case—requires special numerical algorithms.

In this paper, different methods for numerical simulation of the light propagation in the Fresnel region were compared. The described methods can be generally divided into two categories. The first category is based directly on the Fresnel integral [Eq. (1)]. The second one is based on the convolution approach.

A direct approach fails for a small propagation distance because of very fast oscillations of the Fresnel factor. Furthermore, the output and input plane coordinates are not equivalent, which leads to a resampling or interpolation operation. An advantage of this method is the relatively short computation time. Only one FFT operation and two complex vector multiplications are necessary.

Table 1 Range of application of the algorithms.

$z>\frac{N_1(\Delta x_1)^2}{\lambda}$ and $z>\frac{M_1(\Delta y_1)^2}{\lambda}$	Direct approach
$z>\frac{N_1(\Delta x_1)^2}{\lambda}$ and $z>\frac{M_1(\Delta y_1)^2}{\lambda}$	DFT/FFT approach
$z\leqslant\frac{N_1(\Delta x_1)^2}{\lambda}$ and $z\leqslant\frac{M_1(\Delta y_1)^2}{\lambda}$	Convolution approach
$z\leqslant\frac{N_1(\Delta x_1)^2}{\lambda}$ and $z\leqslant\frac{M_1(\Delta y_1)^2}{\lambda}$	Modified convolution approach (for embedded $2N_1\times 2N_2$)

Table 2 Comparison of the algorithms.

	Near* Region	Far* Region	Neighboring Vectors	Computation Effort	Coordinate Scalling
Direct approach	−	+	No	High	User defined
DFT/FFT approach	−	+	Disturbance	Low	Varies with z
Convolution approach	+	−	Disturbance	Medium	1:1
Modified convolution approach	+	+	No	Medium	1:1

*Distances are defined in Table 1.

The convolution approach also enables the numerical calculation of the light complex amplitude in the Fresnel region. It is especially attractive for small and very small distances. A significant advantage of the method is the equivalence of the input and output plane coordinates. However, twice FFT operation is used, which results in prolongation of the computation time.

Additionally, a new modification of the convolution method was proposed. For the propagation calculation, a double-length vector for the convolution operation is used. According to the wavelength, sampling frequency, and number of samples, the maximal propagation distance for one step can be calculated. The whole propagation distance is divided into single steps. The modified convolution approach coincides very well with the experiment and enables us to reduce aliasing errors. A significant disadvantage of this method is the influence of the vector swapping. This effect is equivalent to the opaque square pupils placed at a constant distance along the optical axis in the optical setup. The diffraction on the edges of the pupils can disturb the output distribution for many steps. Long computation time—two FFTs on the double-length vector—is also a considerable disadvantage.

Moreover, the modified convolution method was successfully applied for many cases. Optical structures for beam shaping for optical fiber sensors and computer-generated holograms composed of a few planes were designed for the Fresnel region. Additionally, the described numerical method was applied to analyze the point spread response, optical transfer function, and imaging simulations of the unconventional imaging elements. In all these cases, numerical results coincide well with the experimental results.

The range of the application of the algorithm is presented in Table 1 and the main features of the compared algorithms are presented in Table 2.

Acknowledgments

This work was supported by Warsaw University of Technology. The authors would like to thank the anonymous referees for valuable advise and comments.

References

1. J. J. Stamnes, *Waves in Focal Regions*, Chap. 8, A. Hilger, Bristol (1986).
2. A. Papoulis, *Systems and Transform with Applications in Optics*, Chap. 8, McGraw-Hill, New York (1968).
3. O. Bryngdahl and F. Wyrowski, ''Digital holography-computer generated holograms,'' in *Progress in Optics*, E. Wolf, Ed., Vol. 28, pp. 1–86, North Holland, Amsterdam (1990).
4. U. Schnars and W. Juptner, ''Direct recording of holograms by a CCD target and numerical reconstruction,'' *Appl. Opt.* **33**(2), 179–181 (1994).
5. M. Bernhardt, F. Wyrowski, and O. Bryngdahl, ''Coding and binarization in digital Fresnel holography,'' *Opt. Commun.* **77**(1), 4–8 (1990).
6. E. Carcole, J. Campos, and S. Bosch, ''Diffraction theory of Fresnel lenses encoded in low-resolution devices,'' *Appl. Opt.* **33**(2), 162–174 (1994).
7. E. Carcole, J. Campos, and S. Bosch, ''Diffraction efficiency of Fresnel lenses encoded in low-resolution devices,'' *Appl. Opt.* **33**(29), 6741–6746 (1994).
8. O. Bryndahl, ''Moire: formation and interpretation,'' *J. Opt. Soc. Am.* **64**, 1287–1294 (1974).
9. D. M. Cottrell, J. A. Davis, T. R. Hedman, and R. A. Lilly, ''Multiple imaging phase-encoded optical elements written as programmable spatial light modulators,'' *Appl. Opt.* **29**(2), 2505–2509 (1990).
10. W. T. Cathey, *Optical Information Processing and Holography*, Wiley, New York (1974).
11. J. W. Goodman, ''Holography,'' *Proc. SPIE* **59**(9), special issue (1971).
12. D. Leseberg, ''Computer-generated three-dimensional image holograms,'' *Appl. Opt.* **31**(2), 223–229 (1992).
13. D. Leseberg, ''Sizable Fresnel-type hologram generated by computer,'' *J. Opt. Soc. Am.* **6**, 229–233 (1989).
14. M. Sypek, ''Light propagation in the Fresnel region. New numerical approach,'' *Opt. Commun.* **116**, 43–48 (1995).
15. J. W. Goodman, *An Introduction to Fourier Optics*, McGraw-Hill, New York (1968).
16. R. Bracewell, *The Fourier Transform and Its Applications*, McGraw-Hill, New York (1965).
17. K. Gniadek, *Optical Information Processing*, PWN, Warsaw (1992) (in Polish).
18. J. W. Cooley and J. W. Tukey, ''An algorithm for the machine calculation of complex fourier series,'' *Math. Comput.* **19**, 1–86 (1965).
19. W. H. Southwell, ''Validity of the Fresnel approximation in the near field,'' *J. Opt. Soc. Am.* **71**, 7–14 (1981).
20. A. M. Steane and H. N. Rutt, ''Diffraction calculations in the near field and the validity of the Fresnel approximation,'' *J. Opt. Soc. Am.* **6**, 1809–1814 (1989).
21. G. W. Forbes et al., ''Algebraic corrections for paraxial wave fields,'' *J. Opt. Soc. Am.* **14**, 3300–3316 (1997).

Biographies and photographs of the authors not available.